Impact of Short-Term Climate Variability on Volatile Organic Compounds Emissions Assessed Using OMI Satellite Formaldehyde Observations

T. Stavrakou[1] [ID], J.-F. Müller[1] [ID], M. Bauwens[1], I. De Smedt[1] [ID], M. Van Roozendael[1] [ID], and A. Guenther[2] [ID]

[1]Royal Belgian Institute for Space Aeronomy, Brussels, Belgium, [2]University of California, Irvine, CA, USA

Abstract A major feedback between climate and atmospheric chemistry lies in the meteorological dependence of the emissions of biogenic volatile organic compounds (BVOCs), precursors of important climate forcers, aerosols, and ozone. Whereas the short-term response of BVOC emissions to meteorological drivers is fairly well simulated by current emission models, it is yet unclear whether models can faithfully predict their response to climate change, given the scarcity of long observation records of BVOC fluxes. Here we take advantage of the high yield of formaldehyde (HCHO) in the oxidation of VOCs and use a long-term spaceborne record of HCHO observations in combination with model simulations to show that (i) HCHO interannual variability is primarily driven by climate through its impacts on photochemistry, vegetation fire occurrence, and above all, biogenic emissions and (ii) the HCHO record validates the interannual variability of biogenic emissions calculated by the state-of-the-art Model of Emissions of Gases and Aerosols from Nature (MEGAN) emission model in vegetated regions.

Plain Language Summary This study is motivated by the incomplete knowledge of a major feedback between climate and atmospheric chemistry lying in the meteorological dependence of the emissions of biogenic volatile organic compounds into the atmosphere. Although the short-term response of biogenic fluxes to meteorological drivers is relatively well established, their long-term response is not yet assessed due to the lack of long-term observation records of biogenic fluxes. Here we address two fundamental questions: (i) Can we assess the long-term response of biogenic fluxes to meteorological fields? (ii) Does a widely used biogenic emission model (MEGAN) provide reliable predictions of how those fluxes might respond to climate change? In this study, and for the first time, the long-term variability of hydrocarbon emission fluxes is assessed by using a long-term spaceborne formaldehyde data set (2005–2015). Analysis of this unique observational record and of multiyear model simulations reveals clear evidence that (i) the observed interannual variability is primarily driven by climate through its impacts on biogenic emissions and photochemistry, (ii) the formaldehyde data record validates the long-term response of biogenic emissions to climate variability predicted by the MEGAN state-of-science biogenic emission model, and (iii) the predicted biogenic emission trends appear consistent with the formaldehyde data record.

1. Introduction

Biogenic volatile organic compounds (BVOCs) play a crucial role in the atmosphere as precursors of tropospheric ozone (Chameides et al., 1988; Seinfeld & Pandis, 1998) and aerosols (Claeys et al., 2004; Hallquist et al., 2009) through intricate mechanisms favored by anthropogenic pollutants (Lin et al., 2013). Furthermore, they influence the oxidant concentrations and therefore the abundance of many compounds including methane, a potent greenhouse gas. BVOCs play, therefore, a key role for air quality concerns and in our understanding of the climate system. Their emissions are strongly dependent on visible radiation fluxes and especially temperature: for example, a 5° C warming is estimated to approximately double the emission rate of isoprene (Guenther et al., 2006). Therefore, these emissions are expected to increase in response of climate change, although this effect might be offset by anthropogenic land use change (Chen et al., 2018) and by the inhibition of isoprene emissions due to increasing CO_2 concentrations (Arneth et al., 2007; Possell & Hewitt, 2011).

The short-term response of BVOC fluxes to meteorological drivers is fairly well described by the current emission models, in particular, the Model of Emissions of Gases and Aerosols from Nature (MEGAN; Guenther et al.,

2006, 2012), as shown by its ability to reproduce the diurnal cycle and day-to-day variability of observed fluxes (Müller et al., 2008; Sindelarova et al., 2014). Longer-term variations are more complex: the emission capacity of plants is affected by phenological changes, by biotic and abiotic stresses, and by the plant adaptation to past environmental conditions (Demarcke et al., 2010; Monson et al., 1994). These effects are partially accounted for in models, but on a limited empirical basis. The adequacy of models for predicting the response of BVOC emissions to climate variability is therefore questionable. Direct model validation is difficult, given the scarcity of long-term records of direct flux measurements. On the other hand, the atmospheric photooxidation of hydrocarbons generates large amounts of formaldehyde (HCHO), of which long spaceborne records of vertically integrated columns are available, in particular, from the Ozone Monitoring Instrument (OMI) spectrometer (De Smedt et al., 2015, 2018). Although methane oxidation constitutes the largest HCHO source at global scale, BVOC emissions and, sporadically, biomass burning are generally dominant over vegetated areas (Palmer et al., 2006; Stavrakou et al., 2009). Spaceborne HCHO has been widely used to constrain the emissions of biogenic (Millet et al., 2008; Palmer et al., 2006; Stavrakou et al., 2015), anthropogenic (Stavrakou et al., 2017; Zhu et al., 2014), and pyrogenic (Bauwens et al., 2016; Stavrakou et al., 2016) VOCs through inversion techniques. Here we use an emission model (MEGAN-MOHYCAN, Guenther et al., 2012; Müller et al., 2008) and a global chemistry-transport model (IMAGES, Guenther et al.,2015, 2016) driven by ERA-Interim ECMWF reanalyses (Dee et al., 2011) in order to assess to what extent and by which mechanisms the observed long-term evolution of HCHO columns is related to climate variability.

2. Methods

2.1. Satellite Formaldehyde Observations

The OMI HCHO tropospheric columns are retrieved using an improved differential optical absorption spectroscopy algorithm (De Smedt et al., 2018). The retrieval comprises two main steps: (1) the fit into the earthshine radiance of the HCHO absorption along the mean light path between the sun and the satellite (the slant column) (2) a radiative transfer calculation of the mean light path in order to transform the slant column into a vertical column for each observation condition (the air mass factor). For weak absorbers like HCHO, an additional step is performed, consisting in the normalization of the tropospheric column using the remote Pacific Ocean as reference region (background correction). The OMI HCHO slant columns are retrieved in the $328.5 - 359$ nm interval using high-resolution cross-sections (Meller & Moortgat, 2000). Air mass factors are calculated using radiative transfer simulations (Spurr, 2008). Clouds are treated using the independent pixel approximation. Observations with cloud fractions larger than 40% are filtered out. No explicit correction is applied for aerosols but the cloud correction scheme accounts for a large part of the aerosol scattering effect (De Smedt et al., 2015). The monthly albedo climatology of Kleipool et al. (2008) at 342 nm is used. Daily a priori HCHO profiles are obtained from the TM5 model (Huijnen et al., 2010). Total column averaging kernels are provided for each pixel, as well as an estimation of the random and systematic errors. The random uncertainty is of the order of 0.8×10^{16} molecule per cm^2 for an OMI pixel. The systematic error remaining on the monthly and regionally averaged column ranges between 20% and 40%. The OMI data set was developed in the framework of the EU FP7 project Quality Assurance for Essential Climate Variables (http://www.qa4ecv.eu).

2.2. The IMAGES CTM

Simulations of atmospheric composition are performed with the IMAGES global chemistry-transport model for $2005 - 2015$ at $2° \times 2.5°$ resolution and 40 vertical levels. The model has been extensively described in past studies (Bauwens et al., 2016; Müller & Stavrakou, 2005; Stavrakou et al., 2009, 2016). It uses prescribed daily average methane fields at $3° \times 2°$ resolution on 34 levels provided by an assimilation of surface data over $2005 - 2015$ by the Copernicus Atmospheric Monitoring System. The performed simulations include

- standard simulation, accounting for all non-methane VOC sources (STD),
- as STD, with fixed biogenic emissions for all years (FBIO),
- as STD, neglecting the biogenic sources (NOBIO),
- simulation ignoring all non-methane VOC sources and accounting only for the methane oxidation source (ME).

The simulations NOBIO and ME use oxidant concentrations (OH, HO_2, NO, NO_2, NO_3, and O_3) calculated in the full model simulation STD.

The chemical mechanism follows Bauwens et al. (2016) with a few adaptations. The reaction kinetics of the hydroxyperoxy radicals from the isoprene+OH reaction has been revised based on recent laboratory findings
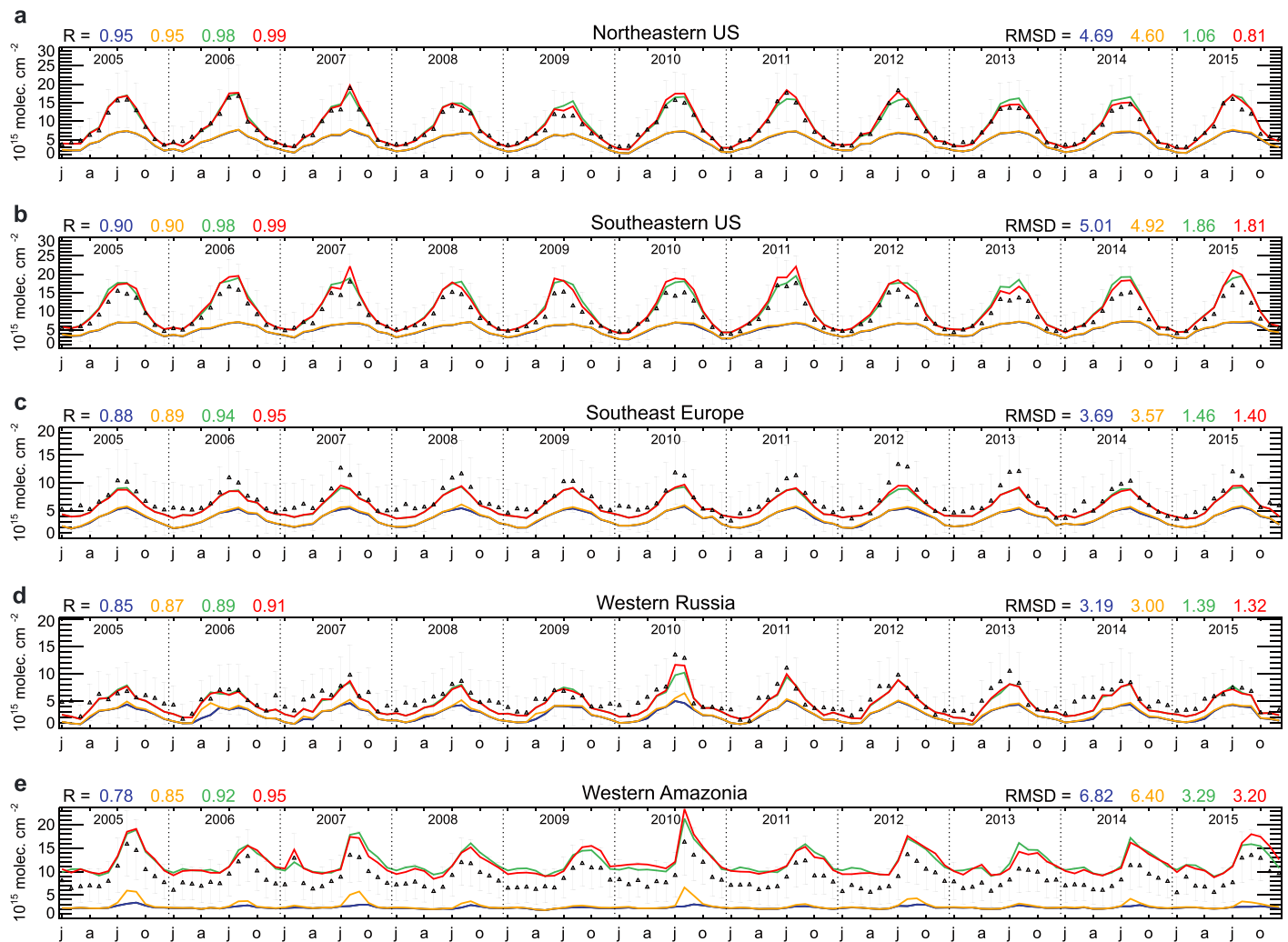
Figure 1. Monthly Ozone Monitoring Instrument and modeled HCHO columns over 2005–2015 averaged over Northeastern United States (a), Southeastern United States (b), Southeast Europe (c), Western Russia (d), and Western Amazonia (e). Observations and uncertainties shown as black symbols and vertical bars. Model results shown for the full simulation (STD, red) and for simulations with identical biogenic fluxes for all years (FBIO, green), with background HCHO formation and biomass burning (NOBIO, orange), and with only background HCHO (ME, blue). Correlation coefficients and RMSDs are given inset. RMSD = root-mean-square deviation.

(Teng et al., 2017). Dihydroperoxycarbonyl peroxy radicals are formed alongside the hydroperoxyenals (HPALDs) following the 1,6 H-shift of the Z-δ-hydroperoxy radicals from isoprene+OH (Peeters et al., 2014). The main fate of the α-hydroperoxycarbonyls formed from these reactions is photolysis (Liu et al., 2018). The reactions of the isoprene hydroxyhydroperoxides and dihydroxy epoxides have been revised (St. Clair, 2016; Bates et al., 2016). When theoretical and laboratory data are lacking, the mechanism is completed based on the Master Chemical Mechanism version 3.3.1 (http://mcm.leeds.ac.uk/MCM).

Anthropogenic VOC emissions are obtained from EDGAR v4.3.2 (Huang et al., 2017) between 2005 and 2012. Anthropogenic emissions of NOx, CO, and SO_2 are taken from HTAPv2 (Janssens-Maenhout et al., 2015). Vegetation fire emissions are obtained from GFED4s (van der Werf et al., 2017). The biogenic emissions of isoprene and monoterpenes are described below. The biogenic methanol source is calculated using MEGANv2.1 for every year multiplied by biogenic emission updates derived by inverse modeling of IASI observations for the year 2009 (Stavrakou et al., 2011).

2.3. Biogenic Emission Modeling

Biogenic emissions of isoprene and monoterpenes are calculated using the MEGANv2.1 model (Guenther et al., 2006, 2012; Stavrakou et al., 2014) coupled with the MOHYCAN multilayer canopy model (Müller et al., 2008). The flux is expressed as
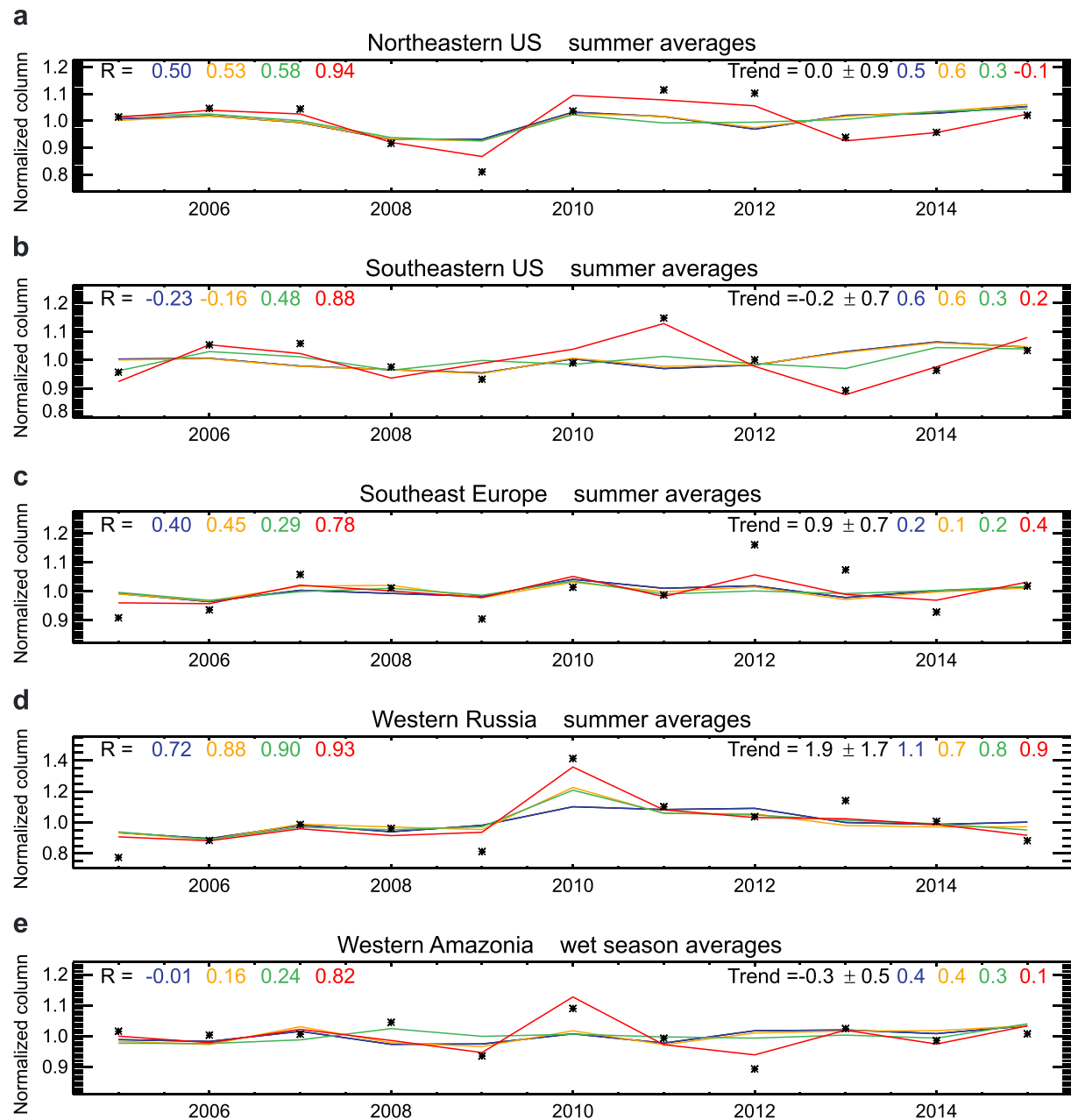
Figure 2. Seasonally averaged Ozone Monitoring Instrument and modeled columns normalized by the mean 2005–2015 seasonal average over (a) Northeastern United States, (b) Southeastern United States, (c) Southeast Europe, (d) Western Russia, and (e) Western Amazonia. Observations and uncertainties shown as black symbols and vertical bars. Model results shown for the full simulation (STD, red) and for simulations with identical biogenic fluxes for all years (FBIO, green), with background HCHO formation and biomass burning (NOBIO, orange), and with only background HCHO (ME, blue). Correlation coefficients and trends (in % per year) are given inset.

$$F = \epsilon \cdot \left[(1 - \mathrm{L}DF) \cdot \gamma_{\mathrm{TLI}} \cdot \gamma_{\mathrm{LAI}} + \mathrm{L}DF \cdot 0.55 \cdot \gamma_{\mathrm{TLD}} \cdot \gamma_{\mathrm{P}} \cdot \mathrm{L}AI \right] \cdot \gamma_{\mathrm{A}} \cdot \gamma_{\mathrm{SM}} \cdot \gamma_{\mathrm{CO_2}}, \qquad (1)$$

where ϵ (mg·m^{-2}·hr^{-1}) is the emission factor under standard conditions and LDF is the light-dependent fraction of the emission (Guenther et al., 2012). The response to temperature (T), solar radiation (P), leaf age (A), soil moisture (SM), CO_2 concentration, and leaf area index (LAI) are accounted for by the activity factors γ. The influence of soil moisture stress is highly uncertain and is neglected here ($\gamma_{SM} = 1$). The effect of CO_2 inhibition is also ignored ($\gamma_{CO_2} = 1$) in view of its large uncertainty: the calculated emission trend due to CO_2 is estimated to range between −0.2% and −0.5% per year during 2005–2015 (Possell & Hewitt, 2011; Wilkinson et al., 2009). The calculation of light attenuation and leaf temperature in the different
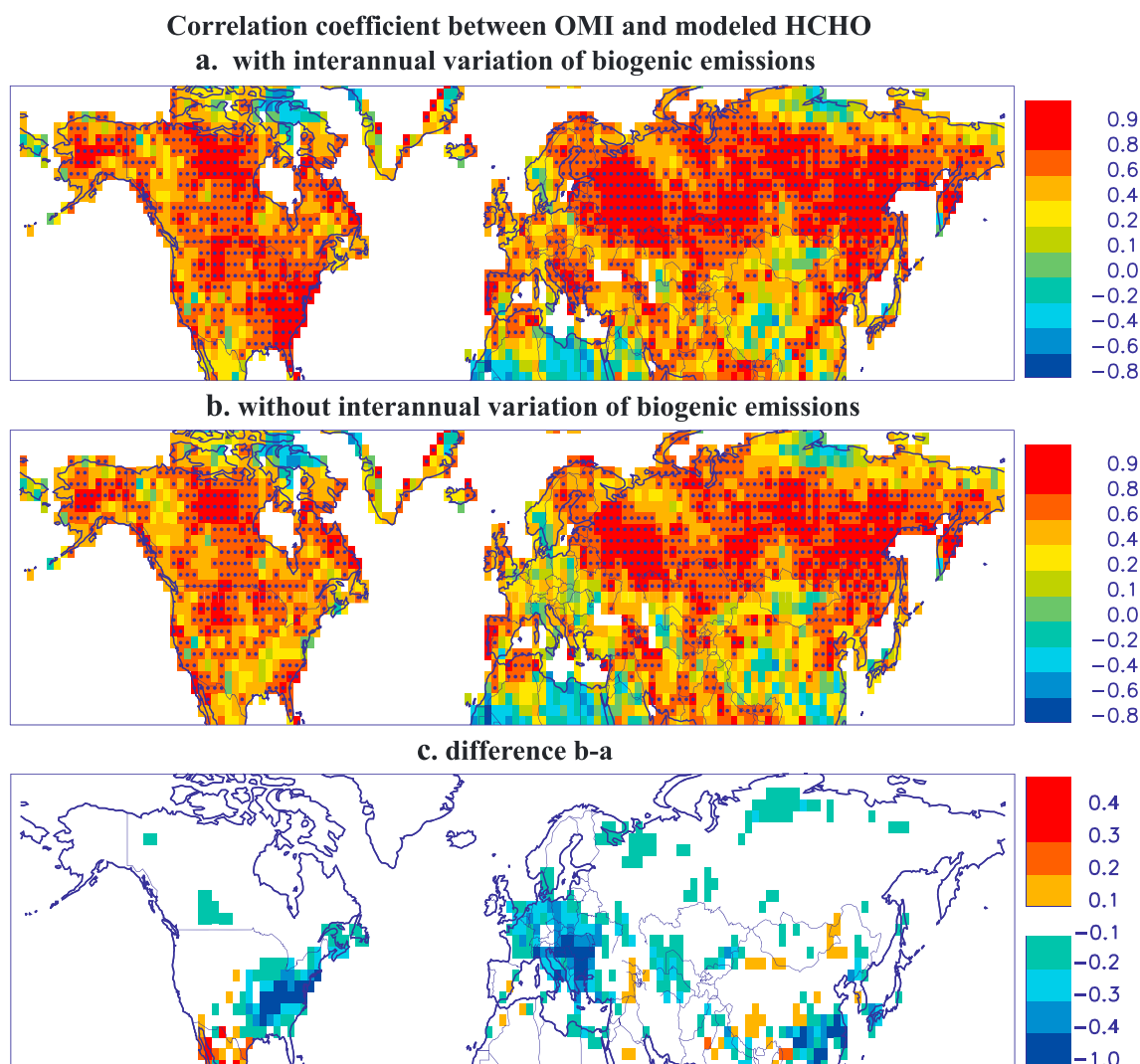
Correlation coefficient between OMI and modeled HCHO
a. with interannual variation of biogenic emissions

b. without interannual variation of biogenic emissions

c. difference b-a

Figure 3. Correlation coefficient (*r*) between summertime (June-July-August) HCHO columns observed by OMI and simulated with IMAGES over 2005–2015 between 25 and 76°N by (a) accounting for the interannual variability of biogenic emissions (STD) and (b) keeping biogenic emissions fixed (FBIO). The stippling shows statistically significant correlation coefficients ($p < 0.05$). The difference of correlation (b)−(a) are shown in (c). OMI = Ozone Monitoring Instrument; HCHO = formaldehyde.

layers follows Müller et al. (2008). The biogenic VOC emission data used in this study are accessible at http://emissions.aeronomie.be.

3. Results

3.1. Seasonal Variability

At midlatitudes over continents, the observed HCHO record displays a marked seasonality (Figures 1 and S2) as both BVOC emissions and background HCHO due to methane oxidation by OH are favored by the warmer and sunnier conditions prevailing in summer. The comparison of full model results with a simulation considering only methane oxidation indicates a substantial contribution of the background, of the order of 50%, which correlates fairly well temporally with the OMI monthly data series ($r \approx 0.8$–0.95, Figure 1). The inclusion of VOC emissions brings the model to an excellent agreement with the data, not only reducing the bias but also improving the temporal correlation of the monthly time series, especially over the Eastern United States ($r \approx 0.99$), where the OMI signal is very strong. Over Amazonia, HCHO is highest during the dry season, when high temperatures and radiative fluxes enhance the productivity of the biosphere (Huete et al., 2006) and of biogenic emissions (Alves et al., 2016) while simultaneously increasing the likelihood of vegetation fires. Methane oxidation plays here only a minor role due to the low levels of nitrogen oxides and hence of OH
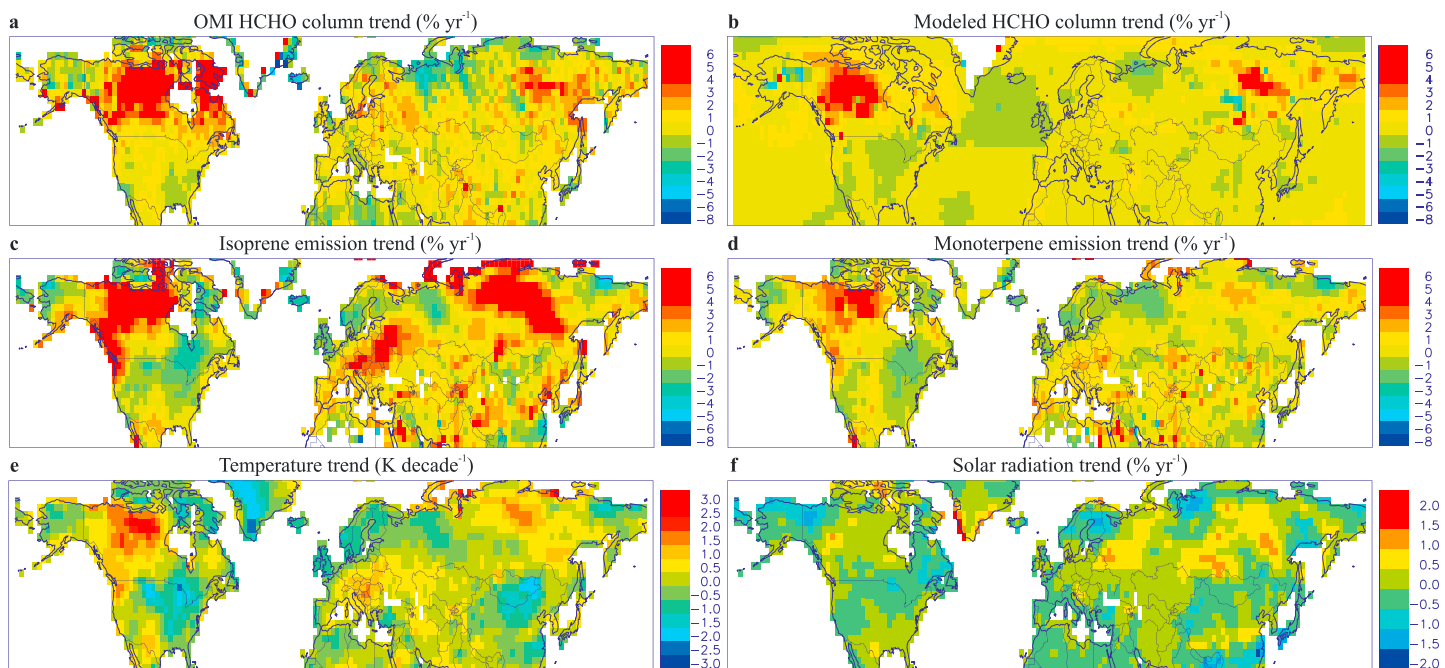
Figure 4. Linear regression trends over 2005–2015 of observed and modeled HCHO columns (% per year) (a,b), isoprene and monoterpene emissions (% per year) (c,d), temperature (K per decade) (e), and solar radiation (% per year) (f). OMI = Ozone Monitoring Instrument; HCHO = formaldehyde.

radicals in the boundary layer (Lelieveld et al., 2016). The impact of fires is generally very small during the wet season (January to April) over Amazonia but also at midlatitudes during the summer, as seen from the comparison of model results neglecting or including biomass burning emissions (Figures 1 and S2). In spite of their very strong regional influence, even the exceptionally intense Russian peat and vegetation fires of July–August 2010 had a much smaller impact than BVOC emissions on average summertime HCHO levels over Western Russia according to our calculations.

Although the modeled columns show both regional underestimations (e.g., over Europe) and overestimations (Amazonia), their excellent temporal correlation with the monthly data series suggests an essentially adequate model representation of the seasonal course of biogenic emissions, in agreement with previous studies (Abbot et al., 2003; Duncan et al., 2009; Palmer et al., 2006; Stavrakou et al., 2015).

3.2. Short-Term Climate Variability and Trends

The interannual evolution of summertime-averaged HCHO columns at midlatitudes — or of wet-season averages in the Tropics — is strongly influenced by the response of biogenic emissions to the short-term climatic variability (Figures 2 and S3), and the calculated impact appears qualitatively and quantitatively consistent with the OMI record. As seen in Figure 3, the simulation ignoring the interannual variability of BVOC emissions correlates poorly with summertime OMI HCHO data at most midlatitudinal regions dominated by biogenic emissions, whereas the inclusion of this variability brings substantial improvements (r increases by 0.1–0.5), in particular, over the Eastern United States, most of Europe, and Southern China. Not only the correlation is greatly improved, to r values of the order of 0.9 over areas with strong emissions (Figures 1 and S2), but also the amplitude of HCHO column variations between favorable (warmer/brighter) and unfavorable years is well captured by the simulation. For example, the temperature jump of almost 3 K between 2009 and 2010 over the Northeastern United States was the main cause for the calculated 50% increase in BVOC emissions (Figure S4a) explaining most of the predicted (and observed) HCHO enhancement by about 25% between these two years, to which a concomitant increase in the background HCHO (by ˜10%) also contributed (Figure 2a). Interestingly, a stronger emission change took place between 2012 and 2013 (decrease by a factor of 1.6), but it led to a smaller HCHO variation (−17%), in agreement with the observations, as the change in background HCHO was of opposite sign to the BVOC emission change (Figure 2). Clearly, the role of background HCHO formation and of its own meteorological dependence should not be overlooked, even though its fluctuations are of lesser amplitude than those of biogenic emissions.

Table 1

2005–2015 Trends and 1-σ Uncertainty Estimates of Observed and Modeled Seasonally Averaged HCHO Columns, Biogenic Fluxes (% per Year) and Temperature (K per Decade) Averaged Over the Regions Defined in Figure S1

Regions	OMI	Model	BVOC	T
Northeastern United States	0.0 ± 0.9	-0.1 ± 0.7	-0.7	-0.8
Southeastern United States	-0.2 ± 0.7	0.2 ± 0.7	0.3	0.2
Northwestern Canada	5.8 ± 1.4	6.5 ± 1.6	4.7	1.7
Western Europe	0.4 ± 0.6	0.5 ± 0.3	-1.7	-0.3
Southeastern Europe	0.9 ± 0.7	0.4 ± 0.3	2.0	0.8
Western Russia	1.9 ± 1.7	1 ± 1.3	1.8	0.2
Southeastern Siberia	1.0 ± 0.9	0.7 ± 1.2	1.5	0.4
Western Amazonia	-0.3 ± 0.5	0.1 ± 0.5	-0.3	-0.1
Eastern Amazonia	-0.1 ± 0.4	0.6 ± 0.5	0.4	0.1
Borneo	-0.3 ± 0.4	0.2 ± 0.4	0.7	0.0

Note. Seasonal averages are calculated over June–August, except for Amazonia and Borneo (January–April). OMI = Ozone Monitoring Instrument; BVOC = biogenic volatile organic compound.

Over the boreal regions of Canada, Alaska, and Siberia, fires account for a large part of HCHO variability, and the excellent model performance in these regions (Figure 3) partly testifies to the quality of the vegetation fire emission inventory (van der Werf et al., 2017), especially at high latitudes (>60°N) where biogenic and biomass burning emissions are of comparable magnitude (e.g., in Northwestern Canada, Figure S2a). Over the more productive southern boreal forest, however, BVOCs contribute much more than open fires to the HCHO columns, by a factor of 5 over Southeastern Siberia (Figure S3c), such that the good correlation ($r = 0.86$) of the simulation ignoring BVOCs with the OMI summertime-averaged columns simply expresses the coincidence of conditions favoring forest fires (hot/sunny weather) with those favoring high biogenic fluxes. Over Western Russia, although the biomass fires peaking in August 2010 did contribute to the spectacular summertime HCHO enhancement observed by OMI (+50% relative to 2009), they were dwarfed by BVOC emissions and by their huge enhancement in 2010 (2.25 Tg, +140% relative to 2009) due to exceptionally warm conditions (+3.6° C, Figure S4). These estimates have their uncertainties, and the fire emissions could possibly be underestimated (Bauwens et al., 2016; Krol et al., 2013), but the dominance of biogenic over pyrogenic fluxes in this region is validated by the timing of the observed peak in July 2010, well captured by the model simulation, whereas fire emissions were highest in August (Figure 1d).

Over Amazonia as well, biomass burning contributes negligibly to HCHO columns during the wet season, except in its Western part in February 2007 (Figure 1e). This month has been excluded from the calculation of the seasonal averages, such that their evolution reflects primarily the BVOC flux variability. Although the climate and particularly temperature are more stable over rainforests than at higher latitudes, fluctuations occur, such as the positive temperature anomaly of 2010 (slightly less than 1° C) which led to substantial enhancements in the calculated BVOC flux (+30% relative to 2009) and in the HCHO seasonal average (+16%), very well captured by OMI data. BVOC flux fluctuations are clearly detected by OMI and are in fairly good agreement with the model over Amazonia and Borneo (Figure S2) despite the relatively low OMI signal and large relative retrieval uncertainties during the wet season.

Even higher correlations (>0.9) are found between modeled and OMI data averaged over the dry season (July–October), when HCHO columns are at their highest (Figure S5). Despite large and highly variable biomass burning fluxes, the biogenic emissions remain indispensable to rationalize the observed evolution of HCHO dry season averages over Amazonia: for example, although pyrogenic emissions in 2007 and 2010 were of comparable magnitude, higher columns were recorded in 2010 (by about 15%), explained by warmer conditions (by ˜0.5° C) and higher BVOC emissions (+20%). By contrast, biogenic emission variability plays a negligible role over Borneo during the dry season, due to the prevalence and extreme variability of fire emissions.

The ongoing climate change is most strongly felt at boreal and arctic latitudes (Cohen et al., 2014), as illustrated by temperature trends exceeding 1 K per decade over Northern Canada and Eastern Siberia over 2005–2015, whereas solar radiation increased by >0.5% per year over large parts of Russia during the same period (Figure 4). These changes led to substantial trends fueled by increasing fire likelihood and by rising biogenic emissions. The model-calculated trends at high latitudes match very well the OMI values, reaching ˜5% per year in Northern Canada and 2% per year over Eastern Siberia, while a regional cooling trend in Northwestern Russia led to a HCHO decline (approximately −1% per year). Elsewhere, the modeled trends are comparatively smaller and in agreement with the observed trends when accounting for their respective uncertainties (Table 1). The overestimations (by 0.4–0.7% per year) found over Amazonia and Borneo are possibly due to the combined effects of deforestation and increasing CO_2 on the emissions (Chen et al., 2018). The CO_2 effect alone is expected to cause a flux decline between −0.2 and −0.5% per year (section 2.3). This effect possibly explains also the trend overestimation (by 0.4% per year) over the Southeastern United States. The trend underestimations over Southeast Europe (0.4% vs. 0.9% per year) and Western Russia (1% vs. 1.9% per year) likely reflect underestimated biogenic emissions (also suggested by the low bias of modeled columns over these regions, Figure 1) and the impact of afforestation in Europe and Western Russia (Chen et al., 2018).

The discrepancy over less productive and drier ecosystems such as Mexico and the Midwestern United States for both the trend (Figure 4) and the correlation (Figure 3) could be related to the neglect of soil moisture stress effect on the emission in the model. A simulation accounting for this factor (γ_{SM}) parameterized using ERA-Interim soil moisture fields (Müller et al., 2008) was performed, but it was found to worsen the temporal correlations over most regions.

4. Conclusions

The long satellite data record reveals clear evidence that HCHO observations reflect climate variability and its trends over regions dominated by biogenic fluxes. The good model prediction of HCHO interannual variability over most temperate and boreal ecosystems as well as over tropical rainforests demonstrates for the first time that the MEGAN model can reproduce the response of biogenic emissions to the changing climate, at least over the timescale of the OMI data record. The model ability to reproduce the observed response of BVOC emissions to climate drivers is crucial for reliable predictions of how atmospheric composition might be impacted by future climate changes.

References

Abbot, D. S., Palmer, P., Martin, R. V., Chance, K. V., Jacob, D. J., & Guenther, A. (2003). Seasonal and interannual variability of North American isoprene emissions as determined by formaldehyde column measurements from space. *Geophysical Research Letters*, *30*, 1886. https://doi.org/10.1029/2003GL017336

Alves, E. G., Jardine, K., Tota, J., Jardine, A., Yanez-Serrano, A. M., Karl, T., et al. (2016). Seasonality of isoprenoid emissions from a primary rainforest in central Amazonia. *Atmospheric Chemistry Physics*, *16*, 3903–3925.

Arneth, A., Miller, P. A., Scholze, M., Hickler, T., Schurgers, G., Smith, B., & Prentice, I. C. (2007). CO_2 inhibition of global terrestrial isoprene emissions: Potential implications for atmospheric chemistry. *Geophysical Research Letters*, *34*, L18813. https://doi.org/10.1029/2007GL030615

Bates, K. H., Nguyen, T. B., Teng, A. P., Crounse, J. D., Kjaergaard, H. G., Stoltz, B. M., et al. (2016). Production and fate of C_4 dihydroxycarbonyl compounds from isoprene oxidation. *Journal of Physical Chemistry A*, *120*, 106–117.

Bauwens, M., Stavrakou, T., Müller, J.-F., De Smedt, I., Van Roozendael, M., van der Werf, G. R., et al. (2016). Nine years of global hydrocarbon emissions based on source inversion of OMI formaldehyde observations. *Atmospheric Chemistry and Physics*, *16*, 10,133–10,158.

Chameides, W. L., Lindsay, R. W., Richardson, J., & Kiang, C. S. (1988). The role of biogenic hydrocarbons in urban photochemical smog: Atlanta as a case study. *Science*, *241*, 1473–1475.

Chen, W. H., Guenther, A. B., Wang, X. M., Chen, Y. H., Gu, D. S., Chang, M., et al. (2018). Regional to global biogenic isoprene emission response to changes in vegetation from 2000 to 2015. *Journal of Geophysical Research: Atmospheres*, *123*, 3757–3771. https://doi.org/10.1002/2017JD027934

Claeys, M., Graham, B., Vas, G., Wang, W., Vermeylen, R., Pashynska, V., et al. (2004). Formation of secondary organic aerosols through photooxidation of isoprene. *Science*, *303*, 1173–1176.

Cohen, J., Screen, J. A., Furtado, J. C., Barlow, M., Whittleston, D., Coumou, D., et al. (2014). Recent Arctic amplification and extreme mid-latitude weather. *Nature Geoscience*, *7*, 627–637.

De Smedt, I., Stavrakou, T., Hendrick, F., Danckaert, T., Vlemmix, T., Pinardi, G., et al. (2015). Diurnal, seasonal and long-term variations of global formaldehyde columns inferred from combined OMI and GOME-2 observations. *Atmospheric Chemistry and Physics*, *15*, 12,519–12,545.

De Smedt, I., Theys, N., Yu, H., Danckaert, T., Lerot, C., Compernolle, S., et al. (2018). Algorithm theoretical baseline for formaldehyde retrievals from S5P TROPOMI and from the QA4ECV project. *Atmospheric Measurement Techniques*, *11*, 2395–2426.

Dee, D., Uppala, S. M., Simmons, A., Berrisford, P., Poli, P., Kobayashi, S., et al. (2011). The ERA-Interim reanalysis: Configuration and performance of the data assimilation system. *Quarterly Journal of the Royal Meteorological Society*, *137*(656), 553–597.

Demarcke, M., Müller, J.-F., Schoon, N., Van Langenhove, H., Dewulf, J., Joó, E, et al. (2010). History effect of light and temperature on monoterpenoid emissions from Fagus sylvatica L. *Atmospheric Environment*, *44*, 3261–3268.

Duncan, B. N., Yasuko, Y., Damon, M. R., Douglass, A. R., & Witte, J. C. (2009). Temperature dependence of factors controlling isoprene emissions. *Geophysical Research Letters*, *36*, L05813. https://doi.org/10.1029/2008GL037090

Guenther, A., Jiang, X., Heald, C. L., Sakulyanontvittaya, T., Duhl, T., Emmons, L. K., & Wang, X. (2012). The Model of Emissions of Gases and Aerosols from Nature version 2.1 (MEGAN2.1): An extended and updated framework for modeling biogenic emissions. *Geoscientific Model Development*, *5*(6), 1471–1492.

Guenther, A., Karl, T., Harley, P., Wiedinmyer, C., Palmer, P. I., & Geron, C. (2006). Estimates of global terrestrial isoprene emissions using MEGAN (Model of Emissions of Gases and Aerosols from Nature). *Atmospheric Chemistry and Physics*, *6*(11), 3181–3210.

Hallquist, M., Wenger, J. C., Baltensperger, U., Rudich, Y., Simpson, D., Claeys, M., et al. (2009). The formation, properties and impact of secondary organic aerosol: Current and emerging issues. *Atmospheric Chemistry and Physics*, *9*, 5155–5236.

Huang, G., Brook, R., Crippa, M., Janssens-Maenhout, G., Schieberle, C., Dore, C., et al. (2017). Speciation of anthropogenic emissions of non-methane volatile organic compounds: A global gridded data set for 1970–2012. *Atmospheric Chemistry and Physics*, *17*, 7683–7701.

Huete, A., Didan, K., Shimabukuro, Y. E., Ratana, P., Saleska, S. R., Hutyra, L. R., et al. (2006). Amazon rainforests green-up with sunlight in dry season. *Geophysical Research Letters*, *33*, L06404. https://doi.org/10.1029/2005GL025583

Huijnen, V., Williams, J., van Weele, M., van Noije, T., Krol, M., Dentener, F., et al. (2010). The global chemistry transport model TM5: Description and evaluation of the tropospheric chemistry version 3.0. *Geoscientific Model Development*, *3*(2), 445–473.

Janssens-Maenhout, G., Crippa, M., Guizzardi, D., Dentener, F., Muntean, M., Pouliot, G., et al. (2015). HTAPv2.2: A mosaic of regional and global emission grid maps for 2008 and 2010 to study hemispheric transport of air pollution. *Atmospheric Chemistry and Physics*, *15*, 11,411–11,432.

Kleipool, Q. L., Dobber, M. R, de Haan, J. F., & Levelt, P. F. (2008). Earth surface reflectance climatology from 3 years of OMI data. *Journal of Geophysical Research*, *113*, D18308. https://doi.org/10.1029/2008JD010290

Krol, M., Peters, W., Hooghiemstra, P., George, M., Clerbaux, C., Hurtmans, D., & Muller, J.-P. (2013). How much CO was emitted by the 2010 fires around Moscow*Atmospheric Chemistry and Physics*, *13*, 4737–4747.

Lelieveld, J., Gromov, S., Pozzer, A., & Taraborrelli, D. (2016). Global tropospheric hydroxyl distribution, budget and reactivity. *Atmospheric Chemistry and Physics*, *16*, 12,477–12,496.

Lin, Y.-H., Zhang, H., Pye, H. O., Marth, W. J., Park, S., Arashiro, M., et al. (2013). Epoxide as a precursor to secondary organic aerosol formation from isoprene photooxidation in the presence of nitrogen oxides. *Proceedings of the National Academy of Sciences of the United States of America*, *110*, 6718–6723.

Liu, Z., Nguyen, V. S., Harvey, J., Müllet, J.-F., & Peeters, J. (2018). The photolysis of α-hydroperoxycarbonyls. *Physical Chemistry Chemical Physics*, *20*, 6970–6979.

Meller, R., & Moortgat, G. K. (2000). Temperature dependence of the absorption cross-sections of formaldehyde between 223 and 323 K in the wavelength range 225–375 nm. *Journal Geophysical Research*, *105*, 7089–7101.

Millet, D. B., Jacob, D. J., Boersma, K. F., Fu, T.-M., Kurosu, T. P., Chance, K., et al. (2008). Spatial distribution of isoprene emissions from North America derived from formaldehyde column measurements by the OMI satellite sensor. *Journal of Geophysical Research*, *113*, D02307. https://doi.org/10.1029/2007JD008950

Monson, R. K., Harley, P. C., Litvak, M. E., Wildermuth, M., Guenther, A. B., Zimmerman, P. R., & Fall, R. (1994). Environmental and developmental controls over the seasonal pattern of isoprene emission from aspen leaves. *Oecologia*, *99*, 260–270.

Müller, J.-F., & Stavrakou, T. (2005). Inversion of CO and NOx emissions using the adjoint of the IMAGES model. *Atmospheric Chemistry and Physics*, *5*, 1157–1186.

Müller, J.-F., Stavrakou, T., Wallens, S., De Smedt, I., Van Roozendael, M., Potosnak, M. J., et al. (2008). Global isoprene emissions estimated using MEGAN, ECMWF analyses and a detailed canopy environmental model. *Atmospheric Chemistry and Physics*, *8*, 1329–1341.

Palmer, P. I., Abbot, D. S., Fu, T.-M., Jacob, D. J., Chance, K., Kurosu, T. P., et al. (2006). Quantifying the seasonal and interannual variability of North American isoprene emissions using satellite observations of the formaldehyde column. *Journal of Geophysical Research*, *111*, D12315. https://doi.org/10.1029/2005JD006689

Peeters, J., Müller, J.-F., Stavrakou, T., & Nguyen, V. S. (2014). Hydroxyl radical recycling in isoprene oxidation driven by hydrogen bonding and hydrogen tunneling: The upgraded LIM1 mechanism. *Journal of Physical Chemistry*, *118*, 8625–8643.

Possell, M., & Hewitt, C. N. (2011). Isoprene emissions from plants are mediated by atmospheric CO_2 concentrations. *Global Change Biology*, *17*, 1595–1610.

Seinfeld, J. H., & Pandis, S. (1998). *Atmospheric chemistry and physics: From air pollution to climate change* (p. 1326). New York: John Wiley & Sons.

Sindelarova, K., Granier, C., Bouarar, I., Guenther, A., Tilmes, S., Stavrakou, T., et al. (2014). Global data set of biogenic VOC emissions calculated by the MEGAN model over the last 30 years. *Atmospheric Chemistry and Physics*, *14*, 9317–9341.

Spurr, R. J. D. (2008). LIDORT and VLIDORT: Linearized pseudo-spherical scalar and vector discrete ordinate radiative transfer models for use in remote sensing retrieval problems. In A. A. Kokhanovsky (Ed.), *Light Scattering Reviews 3* (pp. 229–275). Berlin, Heidelberg: Springer.

St. Clair, J. M. (2016). Kinetics and products of the reaction of the first-generation isoprene hydroxy hydroperoxide (ISOPOOH) with OH. *Journal of Physical Chemistry A*, *120*, 1441–1451.

Stavrakou, T., Guenther, A., Razavi, A., Clarisse, L., Clerbaux, C., Coheur, P.-F., et al. (2011). First space-based derivation of the global atmospheric methanol emission fluxes. *Atmospheric Chemistry and Physics*, *11*, 4873–4898.

Stavrakou, T., Müller, J.-F., Bauwens, M., & De Smedt, I. (2017). Sources and long-term trends of ozone precursors to Asian pollution. In I. Bouarar, et al. (Eds.), *Air Pollution in Eastern Asia: an integrated perspective, ISSI Scientific Report Series 16* (pp. 167–189). Springer International Publishing. https://doi.org/10.1007/978-3-319-59489-7-8

Stavrakou, T., Müller, J.-F., Bauwens, M., De Smedt, I., Lerot, C., Van Roozendael, M., & Song, Y. (2016). Substantial underestimation of post-harvest burning emissions in the North China Plain revealed by multi-species space observations. *Scientific Reports*, *6*, 32307. https://doi.org/10.1038/srep32307

Stavrakou, T., Müller, J.-F., Bauwens, M., De Smedt, I., Van Roozendael, M., De Mazière, M., et al. (2015). How consistent are top-down hydrocarbon emissions based on formaldehyde observations from GOME-2 and OMI*Atmospheric Chemistry and Physics*, *15*, 11,861–11,884.

Stavrakou, T., Müller, J.-F., Bauwens, M., De Smedt, I., Van Roozendael, M., Guenther, A., et al. (2014). Isoprene emissions over Asia 1979-2012: Impact of climate and land use changes. *Atmospheric Chemistry and Physics*, *14*, 4587–4605.

Stavrakou, T., Müller, J.-F., De Smedt, I., Van Roozendael, M., van der Werf, G. R., Giglio, L., & Guenther, A. (2009). Evaluating the performance of pyrogenic and biogenic emission inventories against one decade of space-based formaldehyde columns. *Atmospheric Chemistry and Physics*, *9*, 1037–1060.

Teng, A. P., Crounse, J. D., & Wennberg, P. (2017). Isoprene peroxy radical dynamics. *Journal of the American Chemical Society*, *139*, 5367–5677.

van der Werf, G. R., Randerson, J. T., Giglio, L., van Leeuwen, T., Chen, Y., Rogers, B. M., et al. (2017). Global fire emissions estimates during 1997–2016. *Earth System Science Data*, *9*, 697–720.

Wilkinson, M. J., Monson, R. K., Trahan, N., Lee, S., Brown, E., Jackson, R. B., et al. (2009). Leaf isoprene emission rate as a function of atmospheric CO_2 concentration. *Global Change Biololgy*, *15*, 1189–1200.

Zhu, L., Jacob, D. J., Mickley, L., Marais, E. A., Cohan, D. S., Yoshida, Y., et al. (2014). Anthropogenic emissions of highly reactive volatile organic compounds in eastern Texas inferred from oversampling of satellite (OMI) measurements of HCHO columns. *Environmental Research Letters*, *9*(114004).